

# Short-term variabilities in X-ray/Optical/UV emission from Seyfert 1 galaxy NGC 4593

Sachindra Naik<sup>1\*</sup>, Main Pal<sup>1,2†</sup>, Neeraj Kumari<sup>1‡</sup>

<sup>1</sup> Physical Research Laboratory, Navrangpura, Ahmedabad - 380009, India

<sup>2</sup> Centre for Theoretical Physics, Jamia Millia Islamia University, New Delhi - 110025, India

**Abstract:** We present results obtained from a detailed multi-band analysis of the Seyfert 1 galaxy NGC 4593. Publicly available *Swift* monitoring observations in optical, ultraviolet and X-ray bands were used in the present work. A total of 185 pointings over a duration of about a month were used to understand the variabilities in emission in optical, ultraviolet, soft and hard X-ray bands. It was found that the source emission in the hard X-ray band (1.5-10 keV range) was highly variable compared to that at longer wavelengths. The variability amplitude decreased gradually from hard X-ray to optical bands. A cross-correlation analysis between light curves in different bands inferred that the observed variation in ultraviolet and optical bands is strongly correlated with the hard X-ray emission. Observed time lag for changes in emission in longer wavelength bands with respect to the hard X-ray emission suggests X-ray reprocessing as the cause of variation. Though the observed lag spectrum follows a 4/3rd power of wavelength, as predicted by the standard disk model, the estimated lags are found to be larger than the lags predicted from the standard disk model. This suggests that the actual disk in NGC 4593 is possibly larger than the standard thin disk. Though similar findings have been reported in NGC 5548 and Fairall 9, simultaneous near-infrared, ultraviolet, soft X-ray and hard X-ray band observations of a sample of AGNs with the 1.2 m telescope of Physical Research Laboratory at Mount Abu, India and first space-based multiwavelength observatory of India - AstroSat will provide significant information on the actual and model predicted sizes of the accretion disk.

**Keywords:** accretion – accretion disks – active galactic nuclei – NGC 4593 – X-rays:galaxies

## 1 Introduction

Active Galactic Nuclei (AGNs) are known to contain an accreting supermassive black hole (SMBH) with mass in the range of  $10^{6-9} M_{\odot}$ , at the centre of the host galaxy. Such AGNs radiate over the entire electromagnetic spectrum, starting from X-ray to radio bands. The radiation from these AGNs is known to be released from the accretion of matter from the surrounding regions onto the central black hole. X-ray emission from the AGNs comprises a significant fraction (about 5 – 40%) of the bolometric emission from these objects (Ward et al. 1987). Observation of rapid variability (in  $\sim$ ks range) in X-ray emission suggests that the origin of the high energy photons is close to the central

---

\*snaik@prl.res.in

†rajanmainpal@gmail.com

‡neerajkumari@prl.res.in

black hole (Pounds et al. 1986). Although the X-ray emission region is localized to a very small region around the SMBH and impossible to resolve with the available instruments onboard X-ray observatories, a detailed and thorough study of timing and spectral characteristics offers ways to indirectly probe these regions in these systems.

The major radiative component in the X-ray band is the power law emission which is understood to be due to the Compton upscattering of thermal photons originating from the accretion disk, in an optically thin hot plasma (Haardt & Maraschi 1991). According to the standard accretion disk model, the temperature at any point in the disk varies inversely as the three-fourth power of the radial distance (Shakura & Sunyaev 1973). In the case of AGNs, the thermal radiation from the inner to outer parts of the accretion disk is generally observed in ultraviolet (UV) to optical bands, respectively (Koratkar & Bales 1999) though sometimes the innermost part of the disk contributes towards the soft X-ray emission (Boller et al. 1996). Though the thermal emission from the thin accretion disk peaks in the UV band (Shakura & Sunyaev 1973), the peak is hardly detectable due to the Galactic absorption along the line of sight. The observed emission at longer wavelengths (UV/optical bands) shows variabilities in wide timescales ranging from hours to years. However, the cause of these observed variabilities in UV/optical emission is not well understood. Though the observed long-term (timescale of thousands of years) variabilities in UV/optical bands can be interpreted as due to the changes in mass accretion rate in AGNs (Marshall et al. 2008), variability timescales of hours to days are too short to be associated with the mass accretion rate change.

Apart from this, the observational evidence of fluctuations in X-ray emission leading the corresponding changes in UV/optical emission suggests that the cause of observed short term UV/optical variabilities in AGNs may not be associated with the changes in the accretion disk. Fluctuations in X-ray emission leading the changes in UV/optical emission can occur if the X-ray photons emitted from the compact corona illuminate the optically thick accretion disk and get reprocessed into UV/optical photons (Krolik et al. 1991). A  $4/3$ rd power of wavelength dependence of the predicted delay ( $\tau \propto \lambda^{4/3}$ ) in reprocessed UV/optical emission with respect to the X-ray emission (Cackett et al. 2007) has been found in multiwavelength studies of several AGNs (Edelson et al. 2017 and references therein). However, there are also cases in which observed fluctuations in UV/optical emission are independent of the changes in X-ray emission (Gaskell 2008). Occasional rapid variations in emission at longer wavelengths compared to the X-ray emission have also been found in certain cases (Arvalo et al. 2009). Therefore, simultaneous multiwavelength monitoring observations are necessary to understand the direct and reprocessed emission from regions around the central black hole.

We have carried out one such study to understand the complex variabilities in the Seyfert 1 galaxy NGC 4593 in several wavelength ranges by using publicly available simultaneous UV/optical/X-ray monitoring observations with the *Swift* observatory. NGC 4593, classified as a Hubble type SBb galaxy at a redshift of  $z = 0.009$  (Strauss et al. 1992), harbours a supermassive black hole of mass in the range of  $10^{6-7} M_{\odot}$  (Denney et al. 2006 and references therein). NGC 4593 has been found to be highly variable in wide frequency ranges viz. X-ray, UV, optical and infrared bands, indicating a compact emitting region around the SMBH (Ursini et al. 2016). Using multi-frequency observations with the *Swift* observatory, we investigate such emitting regions around the SMBH in NGC 4593. The followed procedures in analysing the monitoring data, results obtained from the analysis and interpretation of the results are described in the following sections.

## 2 Observation, Data Analysis and Results

Publicly available simultaneous monitoring UV, optical and X-ray observations of NGC 4593 with the *Swift* observatory starting from 2016 July 13 to 2016 August 5 were used in our analysis. Standard procedures were followed to reduce the data acquired simultaneously with the Ultraviolet/Optical

Telescope (UVOT; Roming et al. 2005) and X-ray Telescope (XRT; Burrows et al. 2005) and described in detail in Pal & Naik (2018). Source and background spectra as well as light curves were extracted from simultaneous UV/optical and X-ray data. These products were used to estimate background corrected source count rates and associated one sigma errors for all the UV/optical filters of each observation. Data points showing unusual variations (dips) in UV/optical light curves, possibly due to bad pixels in the detector and data points showing 15% or more variability compared to the local mean were removed from the analysis. This resulted in 173-184 usable points from the UVOT filters that are simultaneous with the data points from XRT. As in the case of UVOT, data from XRT were reduced and net count rates for each observation were extracted by using the total exposure time of respective observations ( $\sim 1$  ks). Average count rates in two X-ray bands (0.3-1.5 keV and 1.5-10 keV) were estimated for each of the XRT observations. A total of 185 usable data points were obtained from the photon counting (PC) mode for both the X-ray bands.

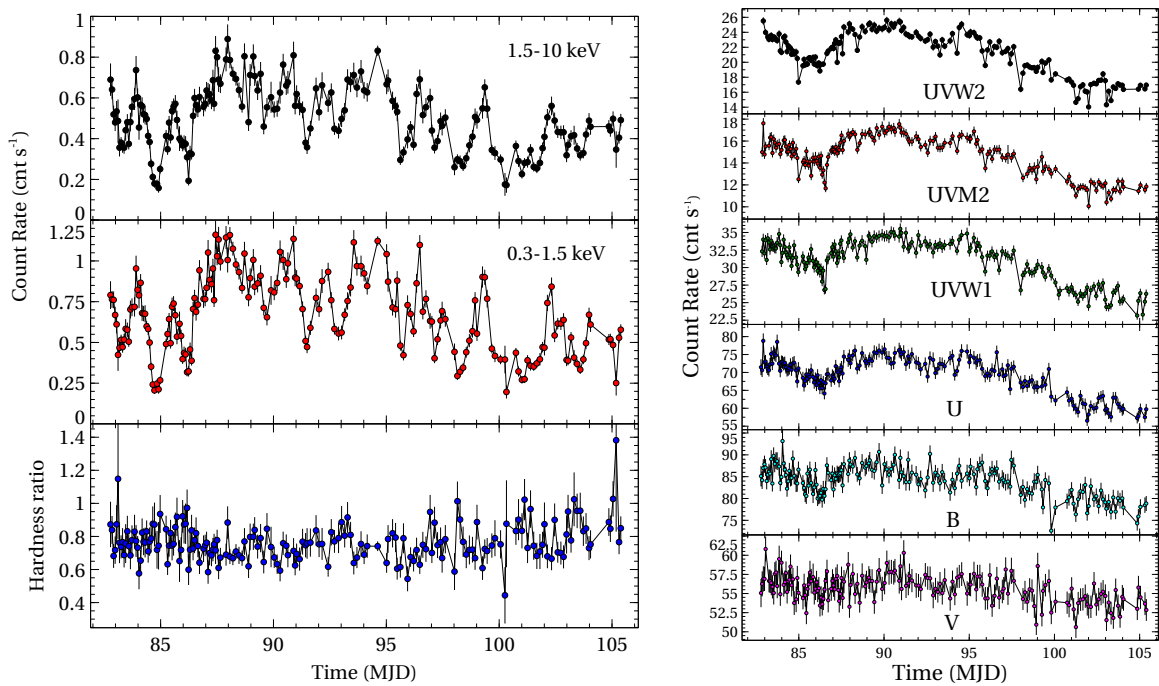


Figure 1: (a) The count rates and hardness ratio for hard and soft X-ray count rates, corrected for systematic effects, observed by *Swift*/XRT in the 1.5-10 keV (top panel), 0.3-1.5 keV (middle panel) bands and their hardness ratio (bottom panel) as a function of time. (b) The count rates of the UV/optical observations simultaneous to X-rays are presented in UVW2, UVM2, UVW1, U, B and V bands from top to bottom as a function of time.

Light curves in 1.5-10 keV (hard X-ray) and 0.3-1.5 keV (soft X-ray) bands were created by using corresponding observed count rates obtained from the *Swift*/XRT observations that are simultaneous with the *Swift*/UVOT observations. The light curves in 1.5-10 keV, 0.3-1.5 keV bands and the hardness ratio (ratio between the light curves in 1.5-10 keV and 0.3-1.5 keV ranges) are shown in top, middle and bottom panels on the left side of Fig. 1, respectively, for all usable observations from 2016 July 13 to 2016 August 5. We consider data in the 1.5-10 keV range as hard X-ray band as the emission in this band is significantly dominated by the power law continuum whereas emission in the 0.3-1.5 keV range is considered as soft X-ray band as it may contain emission from several components such as warm absorption along the line of sight, blurred reflection, intrinsic disk Comptonization. Seyfert type 1 AGNs such as NGC 4593 normally show an excess over power law continuum in soft X-ray band. This is called as “soft X-ray excess”. This component has been explained by various ways.

Under extreme physical conditions (i.e., strong gravity and relativistic effects) close to the black hole, smearing of emission lines in soft X-ray band may produce this excess. This is known as blurred reflection. A component of plasma embedded in the inner disk may also produce this excess and the process involved is called as the disk Comptonization. The warm absorbers in soft X-ray band (0.3-1.5 keV) are associated with the X-ray source. All these components mostly affects the soft X-ray band of the spectrum. The ionized warm absorber with column density of  $10^{20-22} \text{ cm}^{-2}$  in the vicinity of the source can reduce the number of photons in the soft X-ray band, resulting in negative offset compared to the hard X-ray photons. Though the neutral absorption due to the hydrogen column in our Milky Way galaxy also affects the soft X-ray band, the energy range affected due to this neutral absorption is below 0.3 keV.

Light curves in UVW2, UVM2, UVW1, U, B and V bands obtained from the UVOT observations that are simultaneous to X-ray bands are presented in top to bottom panels, respectively, on the right side of Fig. 1. From the figure, it can be seen that the X-ray emission from the AGN varies by a factor of  $\sim 5$  in a few days time and also varies by a factor of  $\sim 2$  in a few hours time. The hardness ratio remains almost constant throughout the duration of the monitoring observations used in this work. The UV and optical light curves appear to be correlated with each other and are also found to be highly variable in days timescale, as in the case of X-rays.

In order to evaluate the dependence of emission in soft bands (soft X-ray and UVW2, UVM2, UVW1, U, B and V bands) on the emission in the hard X-ray band of NGC 4593, we fitted each soft band light curve separately with the hard X-ray light curve with a line  $y = m x + c$ , where  $m$  is the slope and  $c$  is a constant. Here, the slope  $m$  provides how strongly the emission in soft band depends on the emission in the hard X-ray band whereas the offset  $c$  provides information about the slowly varying component in the soft band. This count-count correlation method was first developed to decompose the stable and variable components present in the observed emission from Cygnus X-1 (Churazov et al. 2001) and later has been used in similar studies in AGNs (Taylor et al. 2003). The results obtained from the count-count correlation analysis are shown in Fig. 2 in which the linear function fitting was carried out by considering each soft band light curve as ordinate ( $y$ ) and the hard X-ray light curve as abscissa ( $x$ ). It was found that the slopes of the linear fits were always positive. This indicates a strong relationship between emission in soft bands and the hard X-ray band in NGC 4593. From this count-count correlation analysis, it was also found that the soft X-ray light curve shows a marginal negative offset whereas all other light curves in the UV/optical bands show a positive offset. The negative offset for the soft X-ray band is possibly due to the effect of absorption of soft X-ray photons by the matter along the line of sight. The positive offsets for the other soft band light curves, however, indicate the presence of a weakly variable disk component. Pearson's correlation coefficient ( $\rho$ ) and the significance of the strength of correlation were determined to quantify the strength of inter-band correlation between longer wavelength bands and the hard X-ray band. The correlation coefficient was found to be in the range of  $\sim 0.29 - 0.94$  from optical/UV to soft X-ray bands with very low probability ( $\sim 1.6 \times 10^{-4} - 2.8 \times 10^{-84}$  for V to soft X-ray band) of chance occurrence.

As the soft band light curves are found to be strongly correlated with the hard X-ray light curve of NGC 4593, we attempted to quantify the presence of lag/lead between the soft band and hard X-ray band light curves. For this purpose, publicly available software such as the JAVELIN code (Zu et al. 2013) and the Z-transformed discrete cross-correlation function (ZDCF; Alexander 1997) were used to estimate the timing information between emission in different bands. While using the JAVELIN code to determine the presence of lag/lead, we considered the hard X-ray band as the first light curve whereas each of the other soft band light curves was assumed as second light curve. The lag distributions of the soft bands with the hard X-ray light curve, obtained from using the JAVELIN code, are shown in Fig. 3. The estimated lags for emission in the soft bands with respect to the hard

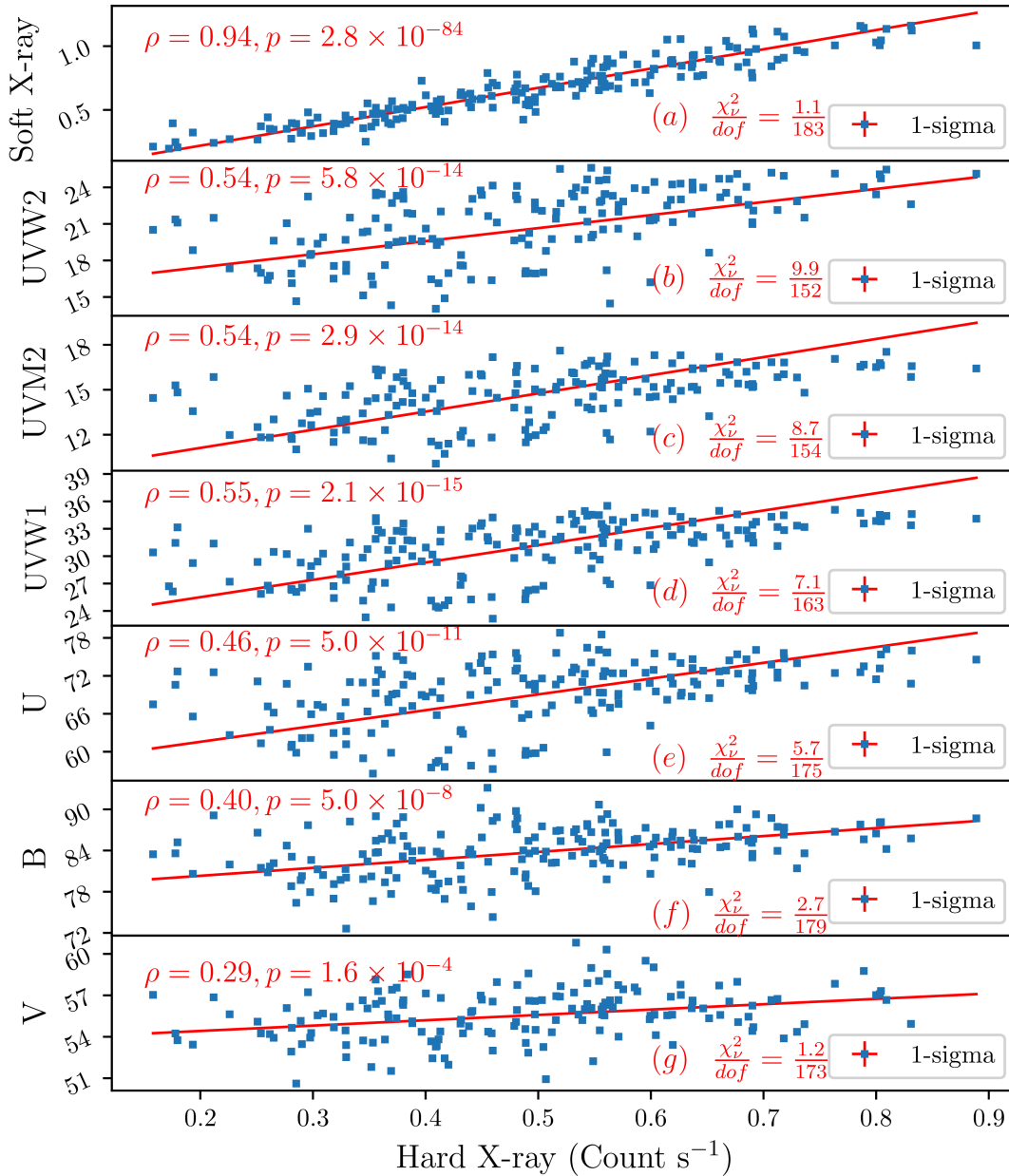


Figure 2: The linear fitting ( $y = m x + c$ , where  $m$  and  $c$  are the slope and a constant, respectively) to the correlation between the soft bands (soft X-ray to V bands) and the hard X-ray band. Here each individual soft band is assumed as the ordinate ( $y$ ) and the hard X-ray band as the abscissa ( $x$ ). The best-fitting line is shown in each of the panels. Best-fitted values of slope and constant for each band are  $1.51 \pm 0.03$  and  $-0.08 \pm 0.02$  (for soft X-ray band),  $20.5 \pm 1.8$  and  $10.9 \pm 0.8$  (for UVW2 band),  $11.1 \pm 1.0$  and  $8.9 \pm 0.5$  (for UVM2 band),  $16.6 \pm 1.5$  and  $22.0 \pm 0.7$  (for UVW1 band),  $24.2 \pm 2.6$  and  $53.9 \pm 1.3$  (for U band),  $11.6 \pm 1.6$  and  $69.0 \pm 0.8$  (for B band) and  $3.7 \pm 0.8$  and  $46.3 \pm 0.4$  (for V band). The  $\chi^2_{\nu}$  represents the reduced  $\chi^2$  values which suggests that the linear fit is not the best fit model for all the inter-band correlations. This seems due to the scatters present here and their origin is not the focus of the paper.

X-ray band are  $0.15 \pm 0.17$  d (soft X-ray band),  $1.51 \pm 1.22$  d (UVW2 band),  $-0.03 \pm 1.20$  (UVM2 band),  $0.4 \pm 1.3$  d (UVW1 band),  $1.47 \pm 1.2$  d (U band),  $0.90 \pm 0.89$  d (B band) and  $1.21 \pm 0.6$  d (V

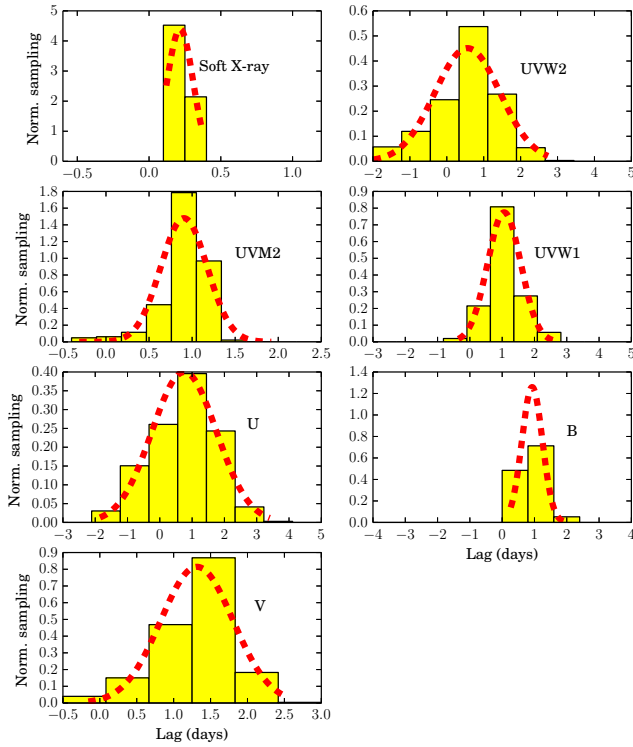


Figure 3: Probability distribution of lags for emission in soft bands (soft X-ray band to V band) with respect to the emission in the hard X-ray band. The red curves in each panel represent the Gaussian representation of probability distribution of the observed lags.

band). These estimated lags between soft bands and the hard X-ray band were also compared with the corresponding values obtained by utilizing ZDCF as described in Pal & Naik (2018). Using ZDCF, the lags for soft X-ray, UVW2, UVM2, UVW1, U, B and V bands with respect to the hard X-ray band, were estimated to be  $-0.12^{+0.22}_{-0.14}$  d,  $0.36^{+0.58}_{-0.13}$  d,  $0.37^{+0.76}_{-0.14}$  d,  $1.41^{+0.43}_{-0.97}$  d,  $1.94^{+1.05}_{-0.88}$  d,  $1.62^{+0.28}_{-0.53}$  d and  $1.63^{+1.35}_{-1.35}$  d, respectively. The error bars are quite large and in some cases the values are consistent with zero or even negative though these estimated lags of soft bands with respect to the hard X-ray band are found to be consistent to those obtained by using the JAVELIN code. Furthermore, there is a clear long-term variability on a month time scale which seems to be related to changes in the accretion rate. The timescale of about a month is too short to observe fluctuations in the accretion rate. Moreover, we do not see any signature of lead in the UV/Optical emission with respect to the X-ray emission as this may not be related to the accretion rate changes.

## 2.1 Lag spectrum

As the lags estimated through ZDCF and JAVELIN for soft bands with respect to the hard X-ray band were comparable, we used the lags determined through ZDCF to create the lag spectrum where lag is a function of wavelength (in nm). The central wavelength for each of the soft bands and the hard X-ray band was used to represent the respective band. The lag spectrum generated by considering estimated lags for each soft band with respect to the hard X-ray band is shown in Fig. 4. We fitted the lag

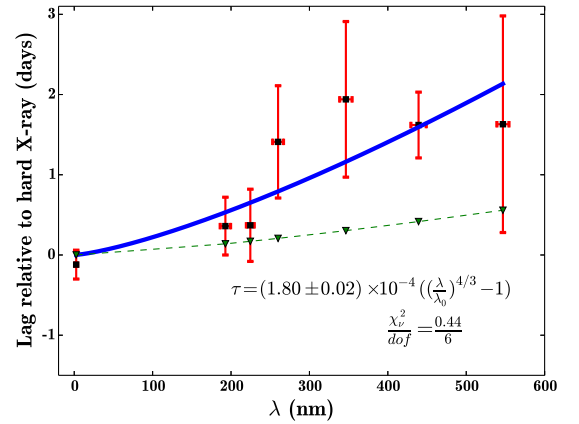


Figure 4: The lag spectrum of NGC 4593 with respect to the emission in the hard X-ray band. The blue curve in the figure represents the best-fit power law model ( $1.8 \pm 0.02 \times 10^{-4} [(\lambda/0.49)^{4/3} - 1]$ ) to the lag spectrum whereas the green dashed curve represents the predicted lag spectrum for the AGN by using the standard accretion thin disk model.

spectrum with a phenomenological power law model for this disk as  $\tau = \alpha \left[ \left( \frac{\lambda}{\lambda_0} \right)^\beta - 1 \right]$ , where  $\alpha$ ,  $\beta$  and  $\tau$  are power-law normalization, power-law index and time delay for a particular wavelength  $\lambda$  with respect to a reference wavelength  $\lambda_0$ , respectively. In the present case,  $\lambda_0 = 0.49$  nm e.g. the central wavelength of the hard X-ray band. The power-law index was fixed at  $4/3$  (according to the standard accretion disk model) as it was difficult to constrain while fitting to the data whereas the normalization was kept free. The best-fit model was found to be  $\tau = (1.80 \pm 0.02) \times 10^{-4} \left[ \left( \frac{\lambda}{0.49} \right)^{4/3} - 1 \right]$  with statistics  $\chi^2_{\nu}/dof = 0.44/6$ .

## 2.2 Lag spectrum predicted from standard accretion disk model

When the accretion disk gets illuminated by X-ray photons from the corona, a fraction of these photons gets absorbed in the disk which then emits at longer wavelengths i.e. UV and optical bands. Therefore, reprocessing of X-ray emission from the hot corona enhances the temperature of the accretion disk. The net temperature of the accretion disk at any radial distance can be expressed as  $T(R) = \left( \frac{3GM\dot{M}}{8\pi\sigma R^3} \left(1 - \frac{R_{in}}{R}\right)^{1/2} + \frac{(1-A)L_x}{4\pi\sigma R_x^2} \cos(\theta_x) \right)^{1/4}$  where  $M$ ,  $G$ ,  $\dot{M}$ ,  $R_{in}$ ,  $R_x$ ,  $L_x$ ,  $A$  and  $\theta_x$  are the mass of the black hole, the gravitational constant, the mass accretion rate, the innermost circular radius, the distance of the disk element from the X-ray source, the bolometric luminosity of the X-ray source, the albedo for X-ray heating and the angle between the normal to the disk surface and the line joining the disk element and the X-ray source, respectively (Cackett et al. 2007). Following the procedure described in Pal et al. (2017) for the conversion of  $R_x$  and cosine of  $\theta_x$  in terms of height  $H$  of the corona from the centre of black hole and radius  $R$  and using the following parameters for NGC 4593 i.e. mass of black hole  $M = 1 \times 10^7 M_{\odot}$ , height  $H = 6r_g$  ( $r_g$  is the gravitational radius), inner radius  $R_{in} = 6r_g$ , albedo  $A = 0.2$ , mass accretion rate in the units of Eddington mass accretion rate  $\dot{m}_E = 0.04$  and bolometric luminosity  $L_x = 10^{43.7}$  erg s<sup>-1</sup> (Vasudevan & Fabian 2009), predicted lags for the central wavelength of each soft band with respect to the hard X-ray band were derived and marked by solid triangles and a green dashed line in Fig. 4. It can be seen that the observed lag for each of the soft band emissions with respect to the hard X-ray band is longer than the expected lag for the corresponding band derived by using the standard accretion disk model.

## 3 Discussion

Using multiwavelength simultaneous monitoring observations of Seyfert 1 galaxy NGC 4593 with the *Swift* observatory, we investigated the observed variabilities in UV/optical and X-ray emission from the AGN. Several techniques were used to study the correlation between soft band (soft X-ray and six UV/optical bands) emission and the hard X-ray emission from the source. Count-count correlation with positive offset was used to find the presence of a marginally variable component in the soft band emission compared to emission in the hard X-ray band. The publicly available ZDCF and JAVELIN codes were used to quantify the presence of lag/delay between the soft band emission with respect to the hard X-ray band. Using the estimated lags for different bands, a lag spectrum was generated and compared with the predicted lag spectrum from the standard accretion disk model. The important findings from this work are summarized below.

- The multiwavelength observations of Seyfert 1 galaxy NGC 4593 showed the presence of short and long term variabilities in all bands as displayed in Fig. 1.
- The count-count plot between the emission in soft bands (soft X-ray and six UV/optical bands) and in the hard X-ray band shows that soft band emission in NGC 4593 is correlated with the

emission in the hard X-ray band (Fig. 2). Presence of a negative offset in the linear fit to the count-count plot for soft and hard X-ray bands suggests that the soft X-ray photons are affected by absorption whereas a positive offset for the UV/optical bands suggests the presence of a weakly variable disk component in the observed UV/optical emission from NGC 4593. Large values of the Pearson coefficient  $\rho$  (0.29 – 0.94) and significantly low values of probability of occurrence by chance ( $10^{-4}$  –  $10^{-84}$ ) suggest that the emission in the UV/optical bands is strongly correlated with the emission in the hard X-ray band.

- Time lag between soft band light curves and the light curve in the hard X-ray band was estimated independently by using the ZDCF and JAVELIN codes and found to be consistent. From cross-correlation analysis, it is found that the changes in the UV/optical emission follow the variations in the hard X-ray emission by  $\sim 0.4 - 1.5$  days. The lag spectrum, generated by using estimated lags for emission in soft bands with respect to the hard X-ray band, indicates that the time lag increases with wavelength. It is well described by a power-law model (4/3rd power of wavelength) as expected from the standard disk model. However, it was found that the predicted lags from the standard accretion disk model are shorter than the observed lags (see Fig. 4) in NGC 4593.

The observed strong correlation between the soft bands and the hard X-ray band suggests that the emission in different bands is related to changes in the accretion flow, Comptonization phenomena or X-ray reprocessing in the accretion disk. The timescale of a month (duration of monitoring observations used in this work) is significantly short compared to the timescale ( $\sim 10^3$  years or more) of fluctuations in the accretion flow in AGNs (Pal et al. 2018). Therefore, the observed short timescale variations in various bands in NGC 4593 can be interpreted as due to inverse Comptonization or X-ray reprocessing in the accretion disk. However, the inverse Comptonization process can be ruled out as in this case, the fluctuations in hard X-ray emission are expected to follow the changes in UV/optical emission whereas the opposite has been observed. The observed lags in UV/optical emission with respect to the hard X-ray emission can be interpreted by the X-ray reprocessing mechanism. Observed short timescale variations are important and interesting to study the coupling between the accretion disk and the corona.

The lags provide information regarding the regions on the accretion disk which emit at various wavelengths. The power-law with an index of 4/3 description of the observed lag spectrum is consistent with the predicted value of the index from the standard accretion disk model (Fig. 4). However, the estimated lags from the standard accretion disk model appear smaller than the observed lags (green dashed line in Fig. 4). It can be seen that the UVW1, U and B bands show clear longer lags than that of the predicted values from the standard disk model while for soft X-ray, UVW2, UVM2 and V bands, the values of estimated and predicted lags marginally agree. Longer values of estimated lags suggest that the size of the accretion disk is larger than the standard accretion disk. The results presented in this work are interesting in a sense that the understanding of the knowledge of a real accretion disk is not complete. The nature of a real accretion disk could be very complex and require simultaneous multiwavelength observations of many such AGNs for a better understanding of the subject. On this regard, we have planned and carried out near-infrared, optical, ultraviolet, soft and hard X-ray observations of a sample of AGNs by using 1.2 m telescope of Physical Research Laboratory at Mt. Abu, Rajasthan, India and the first multiwavelength space-based observatory of India, AstroSat. We expect to derive some important results from this multiwavelength campaign and provide information on the actual size of the accretion disk in these kind of objects.

## **Acknowledgements**

We thank the anonymous referee for his/her useful comments which improved the presentation of the paper. The research work at Physical Research Laboratory is funded by the Department of Space, Government of India. This research has made use of the archival observations of the Swift observatory and XRT Data Analysis Software (XRTDAS) developed under the responsibility of the ASI Science Data Center (ASDC), Italy. SN acknowledges the partial support received from the BINA projects with references DST/INT/Belg/P-02 (India) and BL/11/IN07 (Belgium). MP is thankful for financial support from UGC, India through DSKPDF program.

## **References**

- Alexander T. 1997, *ASSL*, 218, 163  
Arvalo P., Uttley P., Lira P. et al. 2009, *MNRAS*, 397, 2004  
Boller T., Brandt W. N., Fink H. 1996, *A&A*, 305, 53  
Burrows, D. N., Hill, J. E., Nousek, J. A. et al. 2005, *SSRv*, 120, 165  
Cackett E. M., Horne K., Winkler H. 2007, *MNRAS*, 380, 669  
Churazov E., Gilfanov M., Revnivtsev M. 2001, *MNRAS*, 321, 759  
Denney K. D., Bentz M. C., Peterson B. M. et al. 2006, *ApJ*, 653, 152  
Edelson R., Gelbord J., Cackett E. et al. 2017, *ApJ*, 840, 41  
Gaskell C. M. 2008, *RMxAC*, 32, 1  
Haardt F., Maraschi L. 1991, *ApJ*, 380, L51  
Koratkar A., Blaes O. 1999, *PASP*, 111, 1  
Krolik J. H., Horne K., Kallman T. R. et al. 1991, *ApJ*, 371, 541  
Marshall K., Ryle W. T., Miller H. R. 2008, *ApJ*, 677, 880  
Pal M., Dewangan G. C., Connolly S. D., Misra R. 2017, *MNRAS*, 466, 1777  
Pal M., Dewangan G. C., Kembhavi A. K., Misra R., Naik S. 2018, *MNRAS*, 473, 3584  
Pal M., Naik S. 2018, *MNRAS*, 474, 5351  
Pounds K. A., Turner T. J., Warwick R. S. 1986, *MNRAS*, 221, 7  
Romig, P. W. A., Kennedy, T. E., Mason, K. O. et al. 2005, *SSRv*, 120, 95  
Shakura N. I., Sunyaev R. A. 1973, *A&A*, 24, 337  
Strauss M. A., Huchra J. P., Davis M. et al. 1992, *ApJS*, 83, 29  
Taylor R. D., Uttley P., McHardy I. M. 2003, *MNRAS*, 342, L31  
Ursini F., Petrucci P.-O., Matt, G. et al. 2016, *MNRAS*, 463, 382  
Vasudevan R. V., Fabian A. C. 2009, *MNRAS*, 392, 1124  
Ward M., Elvis M., Fabbiano G. et al. 1987, *ApJ*, 315, 74  
Zu Y., Kochanek C. S., Kozowski S., Udalski A. 2013, *ApJ*, 765, 106